Time Evolution of Endpoint Energy of Bremsstrahlung Spectra and Ion Production from an Electron Cyclotron Resonance Ion Source

T. Ropponen*, P. Jones, T. Kalvas, H. Koivisto, P. Peura, JYFL
O. Tarvainen, Los Alamos National Laboratory
P. Suominen, Prizztech Ltd / Magnet technology centre

Abstract

Electron cyclotron resonance ion sources (ECRIS) [1] are used to produce high charge state heavy ion beams for the use of nuclear and materials science, for instance. The most powerful ECR ion sources today are superconducting. One of the problems with superconducting ECR ion sources is the use of high radio frequency (RF) power which results in bremsstrahlung radiation adding an extra heat load to the cryostat. In order to understand the electron heating process and timescales in the ECR plasma, time evolution measurement of ECR bremsstrahlung was carried out. In the measurements JYFL 14 GHz ECRIS was operated in a pulsed mode and bremsstrahlung data from several hundred RF pulses was recorded. Time evolution of ion production was also studied and compared to one of the electron heating theories. To analyse the measurement data a C++ program was developed. Endpoint energies of the bremsstrahlung spectra as a function of axial magnetic field strength, pressure and RF power are presented and ion production timescales obtained from the measurements are compared to bremsstrahlung emission timescales and one of the stochastic heating theories.

DATA ACQUISITION SYSTEM AND DATA ANALYSIS

In order to study the time evolution of bremsstrahlung radiation JYFL 14 GHz ECRIS was operated in pulsed mode. The trigger signal for the RF pulse (leading edge) was synchronized with the data acquisition system. The duration of RF pulses launched into the plasma chamber was set to 1.76 seconds with 5.92 seconds off-time between consecutive pulses. The TTL type reference signal controls the RF switch which has a switching time of 40 ns (0–100 %) and provides timing signal for both the digital oscilloscope (used to record ion beam currents) and the digital signal processing unit (TNT2) [2]. The RF switch controls the 14 GHz oscillator signal to the klystron and a germanium detector was used to measure the radial bremsstrahlung spectra. TNT2 unit generates the data in binary format and a computer is used to store the data. Energy resolution of the germanium detector was 4.2 keV at peak energy of 444 keV and 7.4 keV at 1048 keV of ^{152}Eu (shaping time was set to 2.0 μs).

The effect of the lead shielding around the collimator was also studied. It was noticed [3] that while adding shielding around the lead collimator changed the count rates and also the shape of the bremsstrahlung spectra the timescales remained the same. The size of the collimator hole (from 0.5 mm^2 to 4 mm^2) was not affecting the spectra and had a insignificant effect on the count rate which means that most of the bremsstrahlung events do not come through the collimator but around it.

Data analysis was done with a self-written C++ program. While the TNT2 unit discarded ADC overflows on-the-fly everything else was left untouched in the raw data. Pile-up events are rejected during the data sorting. Typical measurement time per one set of ECR parameters was 90 minutes resulting in data from over 700 RF pulses. To analyze the data 680 RF pulses are used in every data set i.e. bremsstrahlung data of 680 different RF pulses are combined in order to obtain enough statistics. Data from a background measurement is used during the data processing and the background spectrum is subtracted from the measurement data. The data sorting code produces a significant amount of data files. Both "RF on" and "RF off" phases are analysed and, for example, spectrum data is written with 2 ms time step (if the first 1500 ms of the RF pulse is used 750 spectra are produced for both "RF on" and "RF off" phases) and total count rate data integrated over the whole energy spectrum (from 15 keV to 600 keV) is generated throughout the whole length of the RF pulse. Typically a 1 GB of ASCII data is sorted in about 30 seconds. However, because the code also generates figures of all the sorted data as well as gif animations (time evolution of the bremsstrahlung spectrum in 2 ms steps) the sorting time per one data set can be significantly increased. A typical time to sort all the 21 data sets that were recorded during the measurements is between 9 and 10 h (Intel C2D E6600, 3 GB RAM). Using parallel computing to analyze the data would be relatively easy, however, the creation of animations can take 3 GB of memory, or even more, depending on the settings of the analysing program meaning that a normal desktop computer does not have enough memory to run parallel data analysing. Rejection of "bad" RF pulses has also been coded into the analyse program. This ensures that possible incomplete or erroneous RF pulses are discarded from the final analyse. The code has been written for *Unix/Linux* environments and requires *Gnu Scientific Library (GSL)*, *Gnuplot* and *Convert* in order to generate the graphs and animations.

* tommi.ropponen@phys.jyu.fi

KEY ISSUES IN THE RADIAL BREMSSTRAHLUNG TIME EVOLUTION MEASUREMENTS

The radial bremsstrahlung measurement from a magnetic pole was chosen because information about the electron energies was wanted and the charged particle flux at the pole is much greater than between the poles (radial port to the chamber). If the detector would have been located between the radial magnetic field poles (or in axial direction) it is believed that the bremsstrahlung events would originate partially from the plasma (movement of the charged particles in the plasma chamber) due to the fact that there is only about 1.5 mm of aluminium between the plasma chamber and surrounding air. Additional measurements with better collimation, measurements between the poles and axial measurements are planned to take place in the future with JYFL 14 GHz ECRIS.

In the radial bremsstrahlung measurements there are quite a few issues that need to be addressed in order to obtain good results. Firstly, the angular distribution of bremsstrahlung events must be understood. In the non-relativistic energies the angular distribution of bremsstrahlung radiation is "double cone like" meaning that bremsstrahlung radiation is produced in both the direction of movement of the incident electron as well as in the opposite direction [4]. The intensity of the bremsstrahlung emission is larger in the direction of propagation of the incident electron than in the opposite direction. However, the bremsstrahlung cone in the opposite direction becomes meaningful when a vast amount of electrons collide with the plasma chamber walls. The angle of incidence between the electrons and the plasma chamber walls affects the spatial distribution of the bremsstrahlung radiation. In ECRIS plasmas the velocity vectors of high energy electrons are typically oriented almost perpendicularly with respect to the magnetic field. This causes the solid angle, into which bremsstrahlung is emitted, to be large on each magnetic pole. Secondly, the bremsstrahlung photons interact with the matter over a long distance (usually several tens of millimeters) and the scattering processes play an important role before the photon can be detected in the detector crystal. It is possible that a photon changes its path significantly in the media and loses therefore its energy. Because a typical ECRIS uses a sextupole structure for the radial magnetic field, it is understood that the bremsstrahlung radiation originating from all of the six magnetic poles contributes to the measurement that is done in the proximity of one of the six poles. Thirdly, the collimator in radial measurements should be located as close to the detector as possible or if the collimator is located close to the plasma chamber of an ECRIS it should cover basically the whole ECRIS surface which is in the solid angle of the detector.

In the measurements presented in this article a collimator close to the ECRIS was used. Lead plates were used to improve the shielding around the collimator. The amount of the shielding as well as the collimator opening was studied along with the time evolution of bremsstrahlung emission and ion production time measurements. The collimator aperture had an insignificant effect on the spectra: the count rate at the germanium detector was basically the same with open and closed collimator. The shielding around the collimator, however, plays an important role in the shape of the spectra. This can be seen from Figure 1 a) where the steady state spectra of argon plasma is presented with two shielding geometries (the original shielding had less lead plates than the latter shielding). There is a clearly visible "hump" at the energies of 175–375 keV in the spectrum that is recorded with the original collimator/shielding geometry. Presumably, the curve with the "hump" is closer to the real shape of the spectra than the curve without any "hump" because the high energy part of the spectra is not attenuated so much. Adding lead plates around the collimator absorbs the higher energy electron population. However, the lower energy part of the spectra is not affected very much while adding shielding next to the collimator as can be seen from Figure 1 a). This could be a result from a situation where the lower energy part of the spectra is coming through a thinner part of the lead plate shielding (on the edges of the shielding) or partly through the ECR coil structure and therefore remains relatively unchanged. The size of the "hump" for different source parameters (argon plasma) is presented in the subfigures b), c) and d) of Figure 1. In subfigure a) the upper curve at 250 keV represents the original shielding and collimator aperture and the lower curve represents the situation after the changes. In b) and d) at 250 keV: the uppermost curve – coil currents of 550/550 A or 690 W, the middle curve – 500/500 A or 500 W and the lowest curve – 470/470 A or 300 W. Changing the neutral gas pressure does not affect the the steady state count rate very much and all the curves overlap (subfigure c). This means also that the "hump" remains unchanged while the pressure is varied from $1.5{\cdot}10^{-7}$ mbar to $3.5{\cdot}10^{-7}$ mbar. However changing the axial magnetic field strength (subfigure b) or RF power (subfigure d) affects the total count rate integrated over the energies from 15 keV to 600 keV. The height of the "hump" (in relative counts / 2 ms) can be compared to the maximum height of the spectra (lower characteristic lead peak). These values are presented in Table 1 from which it can be seen that increasing the axial magnetic field strength (lowering the gradient) increases the "hump"/max (H/M) relation by over 10 percent. While the RF power is increased the H/M relation increases again 10 percent. The "hump" is growing while magnetic field gradient is lowered or RF power is increased meaning that the amount of hot electrons is increased inside the ECRIS plasma chamber. It has been reported that the effect from increasing the magnetic field (decreasing the distance between the resonances) is comparable to increasing the RF power in terms of heating efficiency [5].

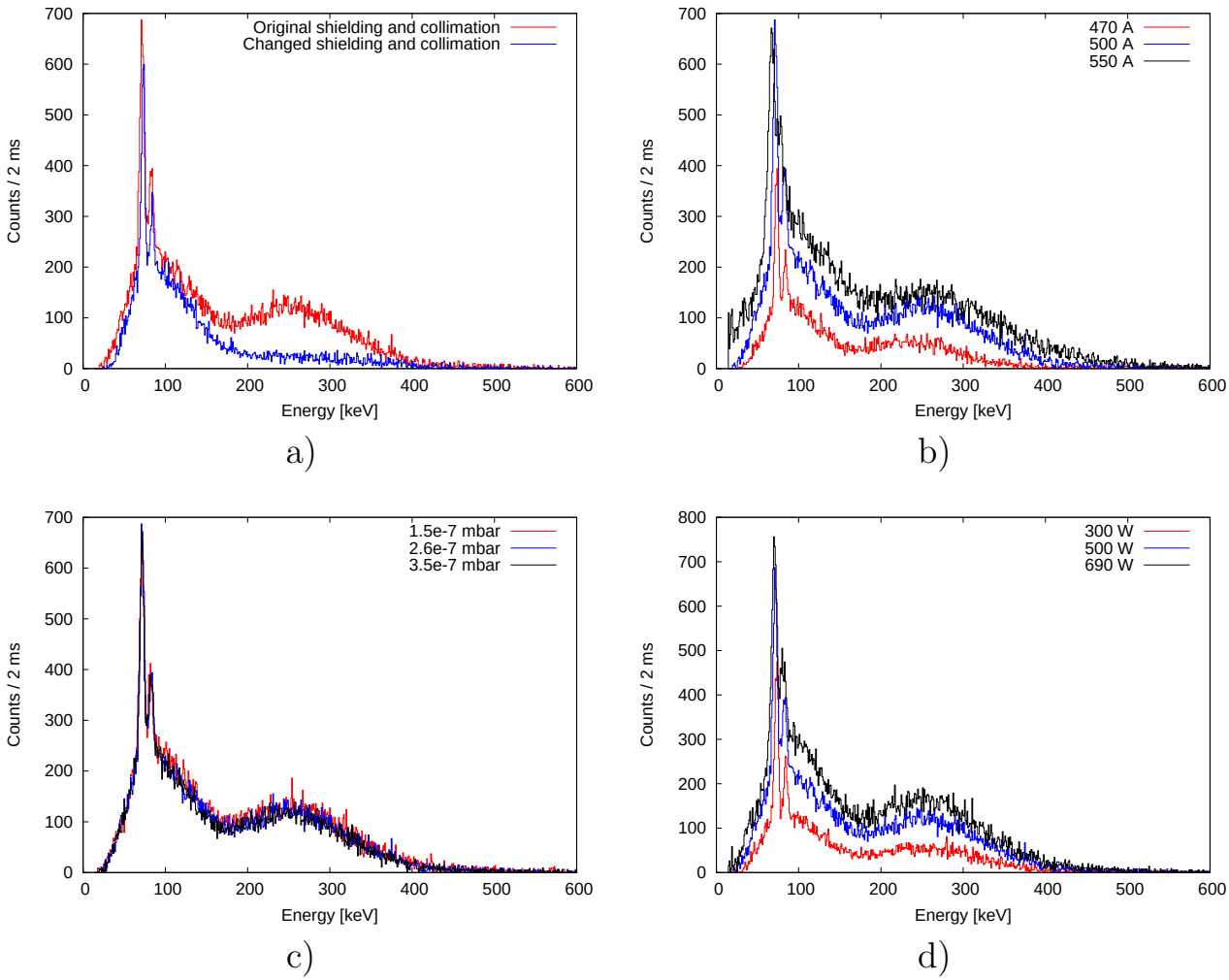

Figure 1: Steady state spectra of argon plasma in a time window of 1500–1502 ms from the leading edge of the RF pulse. a) different shielding and opening of the collimator, b) as a function of axial magnetic field strength, c) as a function of neutral gas pressure, d) as a function of RF power.

EXPERIMENTAL RESULTS

The time evolution of ECR bremsstrahlung emission has been presented as a function of the axial magnetic field, neutral gas pressure and RF power in the references [3] and [6]. The latter includes also the time evolution of argon ion production from the beginning of the RF pulse with some argon charge states. In this section the time evolution of the endpoint energy of the bremsstrahlung emission spectra is presented as a function of the axial magnetic field strength, neutral gas pressure and RF power. The time evolution of oxygen and argon ion production is also presented during the whole RF pulse and the timescales are compared to the bremsstrahlung emission timescales.

Endpoint energy of the bremsstrahlung spectra as a function of axial magnetic field strength, neutral gas pressure and RF power

Table 2 lists the endpoint energies with different ECRIS parameters for argon plasma. The endpoint energies in the steady state phase has been calculated using the following method: 5 % of the maximum count rate in the spectra (75 keV characteristic peak of lead) between times of 1500 and 1502 ms is used as a threshold value. When the average of nine consecutive count rates (each corresponding a single 1 keV energy window) in the aforementioned time window drops below the threshold the median energy corresponding to these nine count rates is defined as the endpoint energy of the spectrum. This is done in order to decrease the effect of statistical behaviour of the count rates.

With argon plasma the endpoint energy of the bremsstrahlung spectra is increasing rapidly when the axial magnetic field gradient is lowered. B_{min} of 0.321 T results

Table 1: Relative count rate at the middle of the "hump" divided by the maximum count rate of the spectra (lower characteristic lead peak) with different ECRIS parameters. Steady state spectra at time window 1500-1502 ms are used (see Figure 1).

	470 A	500 A	550 A	300 W	500 W	690 W
Max / "hump"	13.5 %	18.2 %	23.7 %	12.2 %	18.0 %	22.5 %

Table 2: Endpoint energies of argon bremsstrahlung spectra between 1500–1502 ms from the RF power triggering (see Figure 1) with different JYFL 14 GHz ECRIS settings.

Argon plasma			
B_{inj} / B_{ext}	1.945/0.901 T	2.011/0.946 T	2.111/1.019 T
Endpoint energy	311 keV	364 keV	417 keV
Pressure	$1.5{\cdot}10^{-7}$ mbar	$2.6{\cdot}10^{-7}$ mbar	$3.5{\cdot}10^{-7}$ mbar
Endpoint energy	372 keV	364 keV	363 keV
RF power	300 W	500 W	690 W
Endpoint energy	338 keV	364 keV	375 keV

in 311 keV and endpoint energies of 364 keV and 417 keV are measured for B_{min} of 0.346 and 0.388 T, respectively. The total increase of the endpoint energy is roughly 34 % while the B_{min} increases less than 20 %.

Increased pressure of neutral argon gas has almost no effect on the endpoint energy. Corresponding endpoint energies are: 372 keV ($1.5{\cdot}10^{-7}$ mbar), 364 keV ($2.6{\cdot}10^{-7}$ mbar) and 363 keV ($3.5{\cdot}10^{-7}$ mbar). The total decrease of the endpoint energy is about 2 % while the pressure is varied about 130 %.

Using an RF power of 300 W results in endpoint energy of 338 keV and energies of 364 and 375 keV are recorded with RF powers of 500 and 690 W, respectively. An increase of RF power by a factor of 2.3 results in an endpoint energy increase of about 11 %.

Timescales of oxygen and argon ion production

Timescales of ion production were measured along with the bremsstrahlung emission with JYFL 14 GHz ECRIS. In the ion production measurements both oxygen and argon plasma were used and the results are presented here (for detailed time evolution of argon ion production see [6]). Operation parameters for the ECR for both oxygen and argon plasmas are presented in Table 3. During the measurements the ion source was tuned to O^{7+}(110 μA) or to Ar^{9+} (117 μA) in CW mode. The sampling rate of the oscilloscope (250 ks/sec) was too low in order to use averaging over the noise period and therefore, the ion current data is averaged over 20 consecutive measurement points in order to decrease the amount of noise which was observed at a frequency of 5 MHz (the source for this remained unknown).

Figure 2 illustrates the ion currents during the whole RF pulse. The curves at 1500 ms are the following: the uppermost curve – total count rate of bremsstrahlung events, the second highest curve – O^{7+}, the middle curve – O^{5+}, second lowest curve – O^{3+} and the lowest curve – O^{2+}. With charge states of 2+ and 3+ a so called preglow effect is seen during the first 4–7 ms. Maximum ion current of O^{2+} during the preglow peak is about 200 μA while the steady state current is about 35 μA. This means that during the preglow there is a boost of about 470 %. With O^{3+} the boost at the preglow maximum is 275 % (225 μA) compared to the steady state current of 60 μA.

The steady state of bremsstrahlung emission is reached at around 600 ms (see the vertical line in Figure 2). If short RF pulses (around 4 to 7 ms) were used the production of lower charge states of oxygen (O^{2+}, O^{3+}) could be increased while the amount of bremsstrahlung radiation would still be lower than in steady state phase. From Figure 2 it is also seen that the lower charge states like O^{2+} and O^{3+} start to build up before O^{5+} and the highest charge state presented (O^{7+}) reaches the steady state current around 500 ms.

Figure 3 illustrates the ion currents of the whole RF pulse can be seen in the case of argon plasma. A vertical line is located at 275 ms to mark the time when steady state of the bremsstrahlung production is reached. The following curves can be distinguished at 1500 ms: the uppermost curve – total bremsstrahlung count rate, the second highest curve – Ar^{10+}, the second lowest curve – Ar^{11+} and the lowest curve – Ar^{6+}. The lowest charge state (Ar^{6+}) starts to rise at 5 ms and the maximum of the preglow peak is located around 8 ms (preglow peaks were also observed with argon charge states of 5+,7+ and 8+ and the data for these is presented in [6]). The maximum of the ion current in the preglow peak of Ar^{6+} is about 75 μA while the steady state ion current is 34 μA (factor of 2.2 difference). The higher charge states (10+, 11+) start to rise when roughly 10 ms has elapsed from the launching the RF power into the plasma chamber. Preglow peak is not observed with these higher charge states because the ion source was tuned to

Table 3: Magnetic field strengths of the JYFL 14 GHz ECRIS in ion production measurements, the corresponding resonance lengths in axial direction, neutral gas pressures and RF powers.

Plasma	B_{inj}	B_{min}	B_{ext}	∇B_{inj}^{res}	∇B_{ext}^{res}	d_{res}	Pressure	RF power
Oxygen	2.026 T	0.353 T	0.962 T	6.038 T/m	5.663 T/m	112.6 mm	$4.3{\cdot}10^{-7}$ mbar	745 W
Argon	1.992 T	0.338 T	0.932 T	6.271 T/m	5.815 T/m	118.8 mm	$4.2{\cdot}10^{-7}$ mbar	515 W

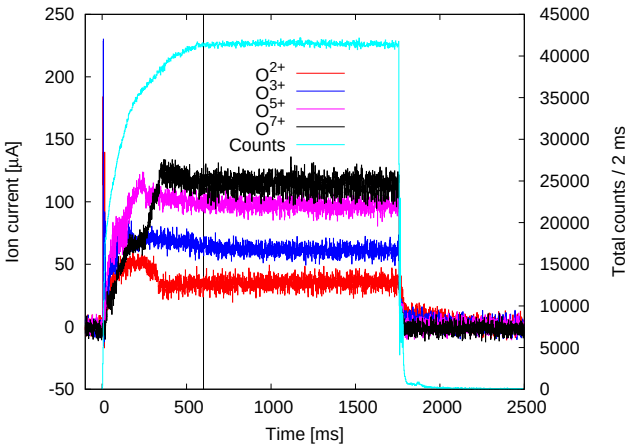

Figure 2: Time evolution of oxygen ions and bremsstrahlung count rate during the whole RF pulse. T=0 corresponds to the leading edge of the RF pulse. A vertical line at 600 ms marks the time when the steady state of bremsstrahlung count rate is reached.

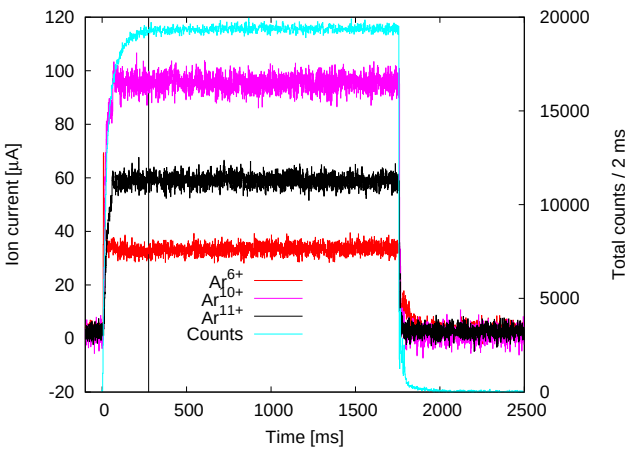

Figure 3: Time evolution of argon ions and bremsstrahlung count rate during the whole RF pulse. A vertical line at 275 ms marks the time when the steady state of bremsstrahlung count rate is reached.

Ar^{9+}. Similar behaviour has been observed in [9].

With argon the ion currents have saturated well before the bremsstrahlung emission saturates. Ion saturation times are roughly 50 ms for Ar^{6+} and about 65 ms for the two higher charge states. The times are significantly lower for argon than oxygen plasma (hundreds of milliseconds, see Figure 2). With oxygen plasma the oxygen atoms can be deposited on the plasma chamber walls and can be released during particle bombardment of the plasma and therefore the time to reach steady state with oxygen plasma could be longer than with argon plasma. However, this needs to be confirmed with additional measurements.

Ion production during the preglow pulse was also studied with argon plasma as a function of the RF power. In this measurement set JYFL 14 GHz ECRIS was tuned with same setting as in the previous measurement and the ion current of Ar^{6+} was observed while varying the RF power from 180 W to 690 W. The following steady state currents for different RF powers were measured: 34 μA (180 W), 33 μA (300 W), 27 μA (500 W), 26 μA (600 W) and 29 μA (690 W). The time evolution of Ar^{6+} ion current for the first 20 ms is presented in Figure 4. At the "peak" the curves are: the lowest curve – 180 W, the second lowest – 300 W, the middle – 600 W, the second highest – 500 W and the highest curve – 690 W. The ion current starts to rise a bit after 4 ms with the two lowest RF powers and with the three highest RF power the rise starts approximately one millisecond later. Reason for this remains unknown. With 180 W there are not a clear maximum in the ion current but with higher RF powers the maximum is well defined. The steady state ion currents are relatively close to each other (from 34 to 26 μA), but the maximum of the preglow peak rises as the RF power is increased. Lowest "peak" current of less than 45 μA is recorded with 180 W and the use of an RF power of 690 W results in the ion current of about 95 μA. Changing the RF power with a factor of 3.8 changes the ion current maximum with a factor of 2.1. After about 20 ms the ion currents are in a steady state phase.

TIMESCALE COMPARISON - MEASUREMENTS VERSUS STOCHASTIC HEATING THEORY

As shown, the steady state of bremsstrahlung count rates is reached in 275 ms with argon plasma and in 600 ms with oxygen plasma. A model by Sergeichev *et al.* [10] is used here to compare the observed timescales to the theory of stochastic electron heating. The model requires information about the magnetic field minimum ($B_{\min}$), microwave power (amplitude of electric field), microwave frequency and the bandwidth of the microwave. According to the heating model the transverse electron energy in the stochastic acceleration regime can be written as

$$W_{\perp}^{0}\,[eV] = DE_0^{\frac{8}{7}} t^{\frac{2}{7}}, \qquad (1)$$

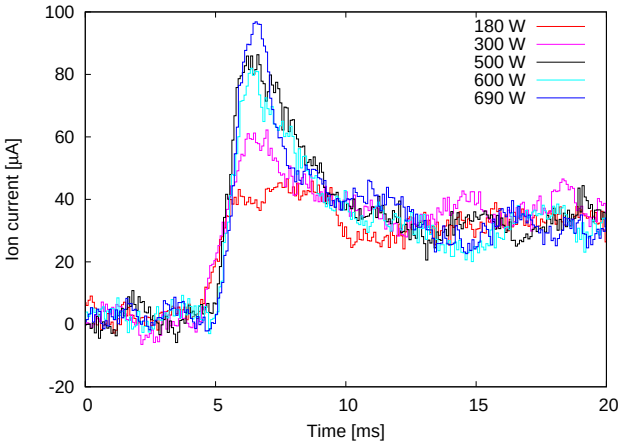

Figure 4: Time evolution of Ar^{6+} during the first 20 ms of the RF pulse with different RF powers.

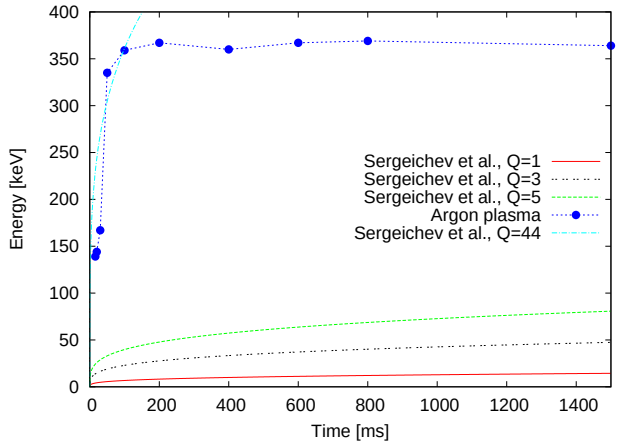

Figure 5: Comparison between the theory of stochastic heating and the endpoint energies measured with JYFL 14 GHz ECRIS. Theoretical curves plotted with different plasma chamber quality factors.

where D is defined as

$$D = \left(\frac{\Delta\omega}{\omega_0}\frac{B_c}{B_c - B_0}\right)^{\frac{4}{7}} \left(\frac{2e}{m}\right)^{\frac{1}{7}} k^{-\frac{3}{7}} \pi^{-\frac{2}{7}}. \qquad (2)$$

In these equations E_0 is the electric field amplitude at the resonance, t time, $\Delta\omega$ frequency bandwidth, ω_0 microwave frequency, B_c resonant magnetic field, B_0 B-minimum and k is derived from the second order axial magnetic field approximation. In the case where the coil currents in JYFL 14 GHz ECRIS are 500/500 A $B_0 = 0.35$ and k is about 147. The klystron of the 14 GHz ECRIS is tuned for a frequency of 14.1 GHz and the reported bandwidth according to the manual is at least 85 MHz. The RF power of 500 W is used thus, the amplitude of the electric field can be calculated approximately using Poynting vector to be about 9.1 kV/m in an empty chamber with plasma chamber quality factor of 1. The stochastic heating model of equation 2 does not explicitly take into account that the resonance field shifts to higher B field as the electrons gain energy (relativistic effect). This shortcome was treated by inserting the functional dependence of the resonance field on the electron energy i.e. $B_c = B_c(W)$ into equation 2 and solving it numerically with a time step of 0.5 ms.

If the value of k is changed from 147 to 139 (corresponding to coil currents of 550/550 A) the maximum energy in stochastic heating according to Sergeichev (Q=1) increases about 0.3 keV (from 14.4 to 14.7 keV). With Q=5 (the amplitude of the electric field is multiplied by 5) the lower value of k (139) produces 1.8 keV higher energy (82.5 keV versus 80.7 keV) than the higher k value after 1500 ms of heating time. Therefore it can be stated that the value of k does not have a major impact on the final maximum energy.

Comparison of timescales between the theory (after Sergeichev) and measurements is presented in Figure 5. Just before 200 ms the lowest curve is after Sergeichev's theory with plasma chamber quality factor of 1, the second lowest curve is theory with Q=3, the middle curve is theory with Q=5, the second highest curve is endpoint energy data from measurements with argon (at given time) and the uppermost curve is calculated from the theory using Q=44. With this very high quality factor the first 100 ms seem to fit relatively well to the measured data, however, after that the Q=44 curve overshoots the measurement values rapidly. This could be due to the fact that the theory does not take into account the limit of stochastic heating, which depends on the group velocity of the EM waves in the plasma. Therefore, the electron energy calculated from the theory does not exhibit saturation behaviour, clearly observed in the measurements, and quality factor Q=44 becomes obsolete after the saturation has been reached. It is suggested that in an empty chamber the quality factor can be in the order of tens or hundreds of thousands [11] and after the plasma has been ignited the quality factor drops down and is around 3 [5]. During the plasma breakdown the quality factor changes rapidly as a function of plasma density (permittivity) but the timescales for this time evolution of quality factor remains unknown. However, another explanation must also be considered. The maximum value of radial magnetic field in the chamber walls of JYFL 14 GHz ECRIS is 0.85 T which corresponds to resonance field for electrons which have energy around 360 keV. The reached steady state behaviour, observed for example in Figure 5, could be a result from a fact that the resonance region has moved into plasma chamber walls and higher energy electrons do not have a resonance zone anymore inside the chamber.

Timescales can be roughly extracted from Figure 5 which presents the time evolution of endpoint energy for the measurement data. The electron energy after 200 ms is about 8 keV according to the stochastic heating theory with plasma chamber quality factor of 1. With Q=3 the energy is 27 keV and with Q=5 the energy is 48 keV at 200 ms. The endpoint energy for argon plasma, using the same 5 % threshold as before, is 367 keV at 200 ms. It

is clear that there are discrepancies between the theory and the measurements. If the quality factor Q is changed the energies according to the theory will increase. However, the timescales from the theory do not match with the measurements: saturation of the endpoint energies is much faster in the measurements than according to the theory where the energies do not saturate at all. Sergeichev's theory does not include any electron energy losses caused by the friction between neutral particles and electrons [10]. These phenomena will, however, decrease the electron energies and some other explanation is needed to explain the measured behaviour.

Different theoretical model for phase regime heating (the electron remains in the accelerating phase all the time) is also presented in [10]. This theory, as expected, generates very high energies in very short time periods. Using the operation parameters from JYFL 14 GHz ECRIS this phase regime theory generates over 1 MeV electrons in 10 ms. These timescales and energies imply that the stochastic heating model needs some corrections (distance between the resonance points, stochastic heating limit) to be accurate and consistent with the measurements and on the other hand rules out the possibility of phase regime heating in an ECR ion source if several resonance crossings are taken into account. This is supported by simulation results reported in reference [12].

DISCUSSION

It is noticed that the steady states for endpoint energies are reached at around 200 ms with argon plasma (see Figure 5). Pressure of the neutral gas inside the ECRIS plasma chamber does not affect the endpoint energy very much. However, the highest endpoint energy (372 keV) is recorded with the lowest neutral gas pressure ($1.5{\cdot}10^{-7}$ mbar). This could be a result from the collision frequency: with the lowest pressures the collision frequency between the particles in the plasma is lowest resulting in longer heating times of electrons before they are collided with other particles or scattered into the radial loss cone of the magnetic field. Changing the RF power from 300 W to 690 W results in an increase of 11 % in endpoint energy. The magnetic field gradient plays, however, an important role in the evolution of endpoint energies. Increasing the axial magnetic field strength (lowering the magnetic field gradient) results into significant changes in the endpoint energy: from 311 keV to 417 keV. Therefore it is stated that the endpoint energy of a bremsstrahlung spectra is dependent on the magnetic field configuration ($B_{\min}$ and gradB) while the effect of the neutral gas pressure and RF power is very small. It is worth of note that the magnetic field generated by the permanent magnets of the JYFL 14 GHz ECRIS is 0.85 T on the magnetic poles. As the electrons gain energy their resonance field shifts towards higher values. Magnetic field value of 0.85 T corresponds to an energy of about 360 keV, which is close to observed endpoint energy of the bremsstrahlung spectra (see e.g. Figure 5). Therefore, it is plausible to claim that the magnetic field profile (and strength) in radial direction may limit the observed energies.

Production times of oxygen and argon ions were also studied and the time evolution of bremsstrahlung emission was compared to times to reach steady state ion currents. A so called preglow effect was observed with O^{2+} and O^{3+} ions. The maximum of the preglow peak ion current in the case of O^{2+} was about 5.7 times the steady state ion current, and with O^{3+} there was a difference by a factor of 3.75. With argon plasma the preglow was observed with Ar^{6+} (and with charge states 5+, 7+ and 8+, see reference [6]). Comparing the steady state of Ar^{6+} to the peak current there is a difference by a factor of 2.2. As expected, the higher charge states build up slower than the lower charge states with both oxygen and argon plasma. The differences in reaching the steady currents with oxygen and argon charge states might be due to more reactive oxygen which is deposited on the plasma chamber walls between the RF pulses and released by ion bombardment during the ignition of the plasma.

The preglow peaks appear several hundreds of milliseconds before the bremsstrahlung emission count rate reaches the steady state. This means that if short millisecond region RF pulses are used bremsstrahlung radiation levels could be decreased relatively more than the ion current, however this needs to be verified with measurements. Typical decay times for a bremsstrahlung spectra from JYFL 14 GHz ECRIS are around tens of milliseconds [3]. Therefore, using an ECR ion source to produce medium (or high, depending on the ECRIS tuning) charge states in a pulsed mode would require RF pulses with a duty factor around 20 % which is very low in terms of continuous ion beam. O^{2+} ion current saturates around 340 ms, O^{3+} and O^{5+} approximately at 700 ms and with O^{7+} it takes nearly 600 ms before the steady state current is reached. The bremsstrahlung count rate reaches the steady state around 600 ms meaning that the ion currents are reaching the steady state before or at same time as the bremsstrahlung emission saturates. With argon plasma the steady state time of the ion currents and the bremsstrahlung emission have a clear difference: Ar^{6+} saturates around 30 ms while Ar^{10+} and Ar^{11+} reaches the steady state ion current after about 70 ms has elapsed from the leading edge of the RF pulse and the bremsstrahlung emission saturates around 275 ms.

Similar behaviour for the ion current rise times with fast sputter sample and gas valve using neon, argon and gold ions have also been reported [13]. However, the ion rise times measured in [13] have been recorded while the ECRIS is in a steady state operation. Rise time for $^{20}Ne^{2+}$ was 1.6 ms and for $^{20}Ne^{8+}$ a rise time of 38.3 ms was measured at 407 W of RF power. In the ion production measurements presented in this article the rise time for O^{2+} is around 5 ms and for O^{7+} the rise time is roughly 20 ms. There are fundamental differences between the measurement setups used with JYFL 14 GHz ECRIS and with ATLAS ECR I (10 GHz). In the measurements presented in

this article, and in the references [3, 6], the ECR plasma was ignited during the RF pulse and turned off with the trailing edge of the RF pulse while the ATLAS ECR I was running in a steady state region with a buffer gas plasma and a fast gas valve or fast sputter sample was used.

When the argon ion production is studied as a function of the RF power it is observed that the maximum ion current of the preglow peak increases with the RF power while the steady state current of Ar^{6+} remained within a few microamperes. The preglow peak starts to rise after about 4 ms (180 W, 300 W) from the launching of the RF power and if higher RF powers (500 W, 600 W, 690 W) are used the rise point is moved to about 5 ms. No explanation for this behaviour has been found yet.

If the stochastic heating theory of Sergeichev *et al.* is compared to the time evolution of endpoint energies measured with JYFL 14 GHz ECRIS it is clear that the theory predicts (with Q=1) energies that are several times lower than the measured endpoint energies are. If the value of Q is increased the energies predicted by the theory will increase but with relatively small Q values the theoretical curves lie at significantly lower energies than the measured values. If Q=44 is used to calculate the electron energy from the theory the first 100 ms are in unison between the measured and theoretical values. After 100 ms the theoretical curve significantly overshoots the measured values. In addition, the timescales from the theory are significantly slower than the timescales obtained from the measurements when a reasonable value for Q is used. In a steady state region the endpoint energies extracted from argon plasma are about 360 keV. Because the timescales that the theory is predicting have a clear discrepancy to the measurement results, it seems that the theory needs some refinement like, for example, adding the stochastic heating limit into the theory.

ACKNOWLEDGMENTS

This work has been supported by the EU 6th Framework programme "Integrating Infrastructure Initiative - Transnational Access", Contract Number: 506065 (EURONS), by the Academy of Finland under the Finnish Centre of Excellence Programme 2006-2011 (Nuclear and Accelerator Based Physics Programme at JYFL) and US Department of Energy under the contract DE-AC52-06NA25396. T. Ropponen would also like to acknowledge financial support from the Graduate School in Particle and Nuclear Physics. The gamma spectroscopy group of JYFL and the use of germanium detector from GAMMAPOOL resource is gratefully acknowledged.

REFERENCES

[1] R. Geller. *Electron cyclotron resonance ion sources and ECR plasmas*. Taylor & Francis, 1996.

[2] L. Arnold, R. Baumann, E. Chambit, M. Filliger, C. Fuchs, C. Kieber, D. Klein, P. Medina, C. Parisel, M. Richer, C. Santos and C. Weber. TNT digital pulse processor. *IEEE Trans. Nucl. Sci.*, 53:723–728, 2006.

[3] T. Ropponen, O. Tarvainen, P. Jones, P. Peura, T. Kalvas, P. Suominen and H. Koivisto. The effect of magnetic field strength on the time evolution of bremsstrahlung radiation created by an electron cyclotron resonance ion source. Submitted to Nucl. Instr. and Meth. A, 2008.

[4] H. W. Koch and J. W. Motz. Bremsstrahlung cross-section formulas and related data. *National bureau of standards*, 31:920–956, 1959.

[5] Y. Jongen. E.C.R. electron acceleration. In *Workshop on the Sixth International ECR Ion Source*, pages 238–255, Berkeley, California, 1985. Lawrence Berkeley Laboratory.

[6] T. Ropponen, O. Tarvainen, P. Jones, P. Peura, T. Kalvas, P. Suominen and H. Koivisto. Time evolution of bremsstrahlung and ion production of an electron cyclotron resonance ion source. To be submitted.

[7] V. M. Povyshev, A. A. Sadovoy, V. P. Shevelko, G. D. Shirkov, E. G. Vasina and V. V. Vatulin. Electron-impact ionization cross sections of H, He, N, O, Ar, Xe, Au, Pb atoms and their ions in the electron energy range from the threshold up to 200 keV. Communication of the Joint Institute for Nuclear Research, Dubna, 2001.

[8] A. Li-Scholz *et al.*. *Atomic data and nuclear data tables.* 36, 1987.

[9] T. Thuillier, T. Lamy, L. Latrasse, I.V. Izotov, A. V. Sidorov, V. A. Skalyga, V. G. Zorin and M. Marie-Jeanne. Study of pulsed electron cyclotron resonance ion source plasma near breakdown: The preglow. In *Proceedings of the 12^{th} international conference on ion sources*, 79, 02A314. Rev. Sci. Instr., 2008.

[10] K. F. Sergeichev, D. M. Karfidov and N. A. Lukina. Electron cyclotron resonance acceleration of electrons to relativistic energies by a microwave field in a mirror trap. *Plasma Physics Reports*, 33:455–473, 2007.

[11] F. Consoli, S. Barbarino, L. Celona, G. Ciavola, S. Gammino and D. Mascali. Investigation about the modes in the cylindrical cavity of an ECR ion source *Radiation Effects and Defects in Solids*, 160:467–475, 2005.

[12] T. Ropponen, O. Tarvainen, P. Suominen, T. K. Koponen, T. Kalvas and H. Koivisto. Hybrid simulation of electron cyclotron resonance heating. *Nucl. Instr. and Meth. A*, 587:115–124, 2007.

[13] R. C. Vondrasek, R. H. Scott, R. C. Pardo and D. Edgell. Techniques for the measurement of ionization times in ECR ion sources using a fast sputter sample and fas gas valve. *Rev. Sci. Instr.*, 73:548–551, 2002.